

Cite this: *CrystEngComm*, 2011, **13**, 3653

www.rsc.org/crystengcomm

## A role for $\pi$ -Br interactions in the solid-state molecular packing of *para*-halo-phenoxy-boronsubphthalocyanines†

Andrew S. Paton,<sup>a</sup> Alan J. Lough<sup>b</sup> and Timothy P. Bender<sup>\*ab</sup>

Received 29th October 2010, Accepted 28th March 2011

DOI: 10.1039/c0ce00796j

We report the synthesis and characterization of a series of *para*-halo-phenoxy-boronsubphthalocyanines (**BsubPcs**). Across this series, a crystal polymorph of *p*-bromophenoxy-**BsubPc** ( $\alpha$ -BrPhO-**BsubPc**) contains a clear and discernible  $\pi$ -Br interaction directing crystallization into a motif not previously seen for phenoxy-**BsubPcs**.

Boron is unique amongst the atoms of the periodic table as only its halides (Cl, Br) template the formation of the trimeric subphthalocyanine (**subPc**) ligand on reaction with phthalonitrile.<sup>1</sup> Researchers have utilized the unique chemical and physical properties of the resulting boronsubphthalocyanine (**BsubPc**) for application in non-linear optics,<sup>2a</sup> organic light emitting diodes (OLEDs),<sup>2b,c</sup> organic field effect transistors (OTFTs),<sup>2d-f</sup> and solar cells.<sup>2g,h</sup> Commonly, the **BsubPc** derivative is used in the solid state and as such an understanding of its solid state molecular packing motifs and methods to influence or even control the motifs are of interest.

Regarding common solid state molecular packing of **BsubPcs**, we have recently highlighted that typical motifs for crystals of phenoxy-substituted boron subphthalocyanines (phenoxy-**BsubPcs**) are the formation of dimers or of ribbons associated through their concave faces.<sup>†</sup> Others have shown that *tert*-butoxy-**BsubPc** and ethoxy-**BsubPc** also form the dimer motif.<sup>4,5</sup> Even one of the few crystal structures of the related alkoxy-tribenzosubporphyrins arranges into a similar concave-face to concave-face dimer motif.<sup>6</sup> Two polymorphs of methoxy-**BsubPc** have been found, one of which possesses the dimeric motif and the other arranges into a ribbon motif associated through the concave faces, not unlike the ribbon structure observed in some phenoxy-**BsubPcs**.<sup>3,7</sup> Peripheral perfluorination of the **BsubPc** ligand on the other hand results in a wholly different motif for the crystal structures of phenoxy-**F<sub>12</sub>BsubPc**<sup>8</sup> and 4-methylphenoxy-**F<sub>12</sub>BsubPc**.<sup>9</sup> This packing structure consists of phenoxy-to-concave-face  $\pi$ -stacking that forms

distinctive 1-dimensional columns of molecules aligned roughly perpendicular to the plane of the **BsubPc** ligand—distinctly different from their corresponding perhydrogenated analogs.<sup>3</sup> In summation, there are two commonly observed motifs for **BsubPc** in the crystalline state: dimeric or ribbon motifs arranged concave-concave common to perhydrogenated derivatives and 1D columns common to perfluorinated derivatives.

Recently, the importance of intermolecular halogen (X) interactions in influencing crystal packing has been recognized. In particular, C-X $\cdots$  $\pi$ , C-H $\cdots$ X, and X $\cdots$ X interactions have been shown to be important in influencing crystal structures. A survey of the Cambridge Structural Database was performed in 2000<sup>10</sup> that searched for the occurrence of C-X $\cdots$  $\pi$  interactions in compounds with a C-X group and at least one 6-membered aromatic group. The study showed that there are particular orientations through which these interactions occur, and that the average distances for these intermolecular C-X $\cdots$  $\pi$  interactions are  $3.224 \pm 0.025$ ,  $3.525 \pm 0.007$ ,  $3.625 \pm 0.009$ , and  $3.698 \pm 0.013$  Å for X = F, Cl, Br, and I, respectively. Specifically, C-Br $\cdots$  $\pi$  and C-I $\cdots$  $\pi$  intermolecular interactions have been shown to mediate a tris-(halophenoxy)triazine and trihalobenzene guest-host inclusion complex, with the trihalobenzene molecule held in channels created by three triazine derivatives.<sup>11</sup> Also, a group of four C-X $\cdots$  $\pi$  (X = Br, I) intermolecular interactions working in concert has been shown to construct a building block for a series of staircase inclusion compounds.<sup>12</sup> The C-H $\cdots$ X and X $\cdots$ X interactions have also been shown to affect the crystal packing structure and solid-state molecular structure of three (2,2'-bipyridine-*N,N*)-dibromo-*cis*-bis[1,1-diphenylhydrazido]-molybdenum(vi) derivatives.<sup>13</sup>

There are three reported crystal structures that suggest halogen-boron or halogen- $\pi$  interactions may influence the crystallization of **BsubPc** derivatives: Cl-**F<sub>12</sub>BsubPc**,<sup>14</sup> Br-**F<sub>12</sub>BsubPc**,<sup>15</sup> and F-**F<sub>12</sub>BsubPc**.<sup>16</sup> Each is arranged in a concave to convex arrangement having halogen-boron distances of 3.671(3), 3.721(3), and 3.228(5) Å, respectively, which are all below the sum of their respective B $\cdots$ X van der Waals radii.<sup>17</sup> However, it is difficult to determine whether this arrangement is formed under the thermodynamic direction of a halogen-boron interaction, a halogen- $\pi$  interaction or rather that it is the preferred crystallization motif of perfluorinated **BsubPcs** based solely on geometric considerations. Additionally, these halo-**BsubPc** derivatives do not offer an opportunity for synthetic variation and thus also do not allow for the examination of the use of halogen-boron interactions to engineer crystals of **BsubPc**.

<sup>a</sup>Department of Chemical Engineering and Applied Chemistry, The University of Toronto, 200 College St., Toronto, Ontario, Canada M5S 3E5. E-mail: tim.bender@utoronto.ca

<sup>b</sup>Department of Chemistry, University of Toronto, 80 St. George St., Toronto, Ontario, Canada M5S 3H6

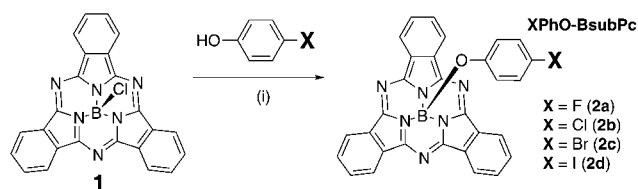
† Electronic supplementary information (ESI) available. CCDC reference numbers 799250–799252, and 814720. For ESI and crystallographic data in CIF or other electronic format see DOI: 10.1039/c0ce00796j

It would be of interest to see whether boron-halogen interactions could be used to crystal engineer **BsubPcs** bearing synthetically variable halogenated fragments preferably resulting in arrangements within the crystal not previously seen. Furthermore, it would be of interest to see evidence to the affirmative or to the contrary of the role of direct halogen–boron or halogen– $\pi$  interactions. Given our recent experience with phenoxy-**BsubPcs**,<sup>3</sup> the incorporation of halogens onto a phenoxy moiety would allow us to study the effect of halogenation as well as have multiple reference structures for comparison. Furthermore, if the carbon spacer is a phenoxy unit or higher aryloxy unit, specific angular (*meta*- and *para*-) and distal options are possible for future studies. In our previous study we synthesized and characterized 4-fluorophenoxy-**BsubPc** (FPhO-**BsubPc**, compound **2a**, Scheme 1). For this derivative there was no evidence of halogen–boron interactions and the derivative crystallized into an arrangement nearly identical to phenoxy-**BsubPc** itself.<sup>3</sup>

In this communication, we wish to report the synthesis, crystallization and characterization of the three additional *para*-halogenated-phenoxy-**BsubPcs**. The syntheses were carried out according to a procedure outlined previously (Scheme 1).<sup>3</sup> Briefly, Cl-**BsubPc** (**1**, Scheme 1) was reacted with the appropriate *para*-halophenol at reflux in toluene. Purification was carried out *via* Kauffman column chromatography on standard basic alumina as the adsorbant and dichloromethane as the eluent yielding compounds **2b–d** (Scheme 1). Finally, all crystallizations were performed *via* vapour diffusion with benzene as the solvent and heptane as the anti-solvent. For compound **2c** a further vapour diffusion crystallization was also performed using dichloromethane as the solvent and pentane as the anti-solvent. In all cases, within one to two weeks, high quality single crystals suitable for X-ray diffraction were grown.

The molecular arrangements within the crystal (extended beyond the unit cell) for 4-chlorophenoxy- (ClPhO-) and 4-iodophenoxy- (IPhO-) **BsubPc** (compounds **2b** and **2d**) are illustrated in Fig. 1b and 1e, respectively. The arrangement of the previously reported FPhO-**BsubPc** is redrawn in Fig. 1a for comparison. As was the case for the solid state molecular packing of FPhO-**BsubPc** (and other *para*-phenoxy-**BsubPcs**),<sup>3</sup> ClPhO-**BsubPc** and IPhO-**BsubPc** orient themselves into distinct dimers; however, each is distinctly different in its arrangement of the dimers relative to one another. Despite the larger size of the iodine atom, IPhO-**BsubPc** arranges into a nearly identical crystal structure as FPhO-**BsubPc** as can be seen by a comparison of Fig. 1a and 1d. In the case of ClPhO-**BsubPc**, while it does organize into discernible dimers, the arrangement of dimers relative to one another is markedly different than in the case of FPhO-**BsubPc** and IPhO-**BsubPc**.

In contrast, when grown from benzene/heptane the crystal structure of BrPhO-**BsubPc** (Fig. 1c) does not show the association of pairs of **BsubPc** molecular fragments into dimers; rather, it is arranged into 1D ribbons of **BsubPc** molecules. The bromine of one



**Scheme 1** Synthesis of *para*-halophenoxy-**BsubPcs** (**2a–d**) from Cl-**BsubPc** (**1**). Conditions: (i) 5 equiv. toluene, reflux, HCl.

molecule is located nearly in the centre of the concave-side of the neighbouring molecule beneath the boron atom (Fig. 1c). A closer examination of the geometry (Fig. 2) shows the separation between the bromine and the boron in the neighbouring molecule is 3.850(5) Å, which is equal to the sum of the van der Waals radii.<sup>17</sup> There is also a measurable C–Br $\cdots$  $\pi$  interaction at a distance of 3.380(5) Å between the bromine and the centroid (Cg) of the concave-side of the five-membered  $\pi$ -ring consisting of C9–C10–C15–C16–N3 of the **BsubPc** (see numbering Fig. S3).<sup>†</sup> Additionally, between the rows of molecules there is a convex-side to convex-side  $\pi$ – $\pi$  interaction between two **BsubPc** molecular fragments at a distance of 3.716(3) Å (Fig. 1c). An examination of the bond angles of this molecule (in particular the B1–O1–C25 angle) reveals no bond angle strain is present. Unlike other cases of phenoxy-**BsubPcs** where the phenoxy molecular fragment is positioned between lobes of the **BsubPc** ligand, in this case it is positioned over a lobe (above N5–C24–C23–C18–C17). This form of BrPhO-**BsubPc** will hereafter be referred to as  $\alpha$ -BrPhO-**BsubPc**.<sup>§</sup> Single crystals of BrPhO-**BsubPc** were also obtained from dichloromethane/pentane diffusion crystallization. In this case a second polymorph was found wherein the solid-state arrangement is again dominated by the formation of discernible dimers and for which the overall arrangement is identical to that obtained for IPhO-**BsubPc** (Fig. 1d). This form of BrPhO-**BsubPc** will hereafter be referred to as  $\beta$ -BrPhO-**BsubPc**.<sup>¶</sup> Using a commercial software package (Materials Studio version 5.0, Accelrys Inc.) we calculated the energy difference between  $\alpha$ -BrPhO-**BsubPc** and  $\beta$ -BrPhO-**BsubPc** to be  $\sim 4.35$  kcal mol<sup>–1</sup>, with  $\beta$ -BrPhO-**BsubPc** being lower in energy. This indicates that each polymorph is relatively close in energy and that  $\alpha$ -BrPhO-**BsubPc** might be kinetically favoured whereas  $\beta$ -BrPhO-**BsubPc** might be thermodynamically favoured (assuming the solvent systems used for growth does not favour one polymorph over the other).

In an effort to explain the uniqueness of BrPhO-**BsubPc** and what structural features might be influencing its formation, we computed the electrostatic potential surface for each of FPhO-**BsubPc**, ClPhO-**BsubPc** and BrPhO-**BsubPc** using the 6-31G\* basis set with the B3LYP DFT method (as implemented in the commercial software package Spartan '06) and IPhO-**BsubPc** using instead the 6-311G\* basis set, the results of which are illustrated in Fig. S9, S10, 3 and S11, respectively.<sup>†</sup> According to these calculations, considering first BrPhO-**BsubPc**, a region of relative electron deficiency is present in the  $\pi$ -system at the boron atom on the underside of the molecule, while a moderate yet noticeable electron surplus is present around the circumference of the bromine atom (Fig. 3). If we consider the spatial arrangement of these two areas of electron deficiency and surplus within the crystal structure, they are oriented in such a way and at a suitable distance (Br–B 3.850 Å and Br– $\pi$  3.380 Å, as mentioned above) to constitute an electrostatic interaction between the bromine atom and the  $\pi$ -system of the **BsubPc** molecular fragment. However, the same electrostatic distribution can also be found in the remaining derivatives (see Fig. S7, S8 and S9 for FPhO-**BsubPc**, ClPhO-**BsubPc** and IPhO-**BsubPc**, respectively).<sup>†</sup> Clearly, it is not simply the electrostatic interaction which is motivating the formation of the unique solid-state molecular packing of  $\alpha$ -BrPhO-**BsubPc**.

Examination and comparison of Fig. S9, S10, 3 and S11<sup>†</sup> will also show the expected change in size of the halogen on going from fluorine to iodine. We are therefore left with the following explanation in an attempt to describe the uniqueness of  $\alpha$ -BrPhO-**BsubPc**: it is not only the electrostatic interaction between the **BsubPc** molecular

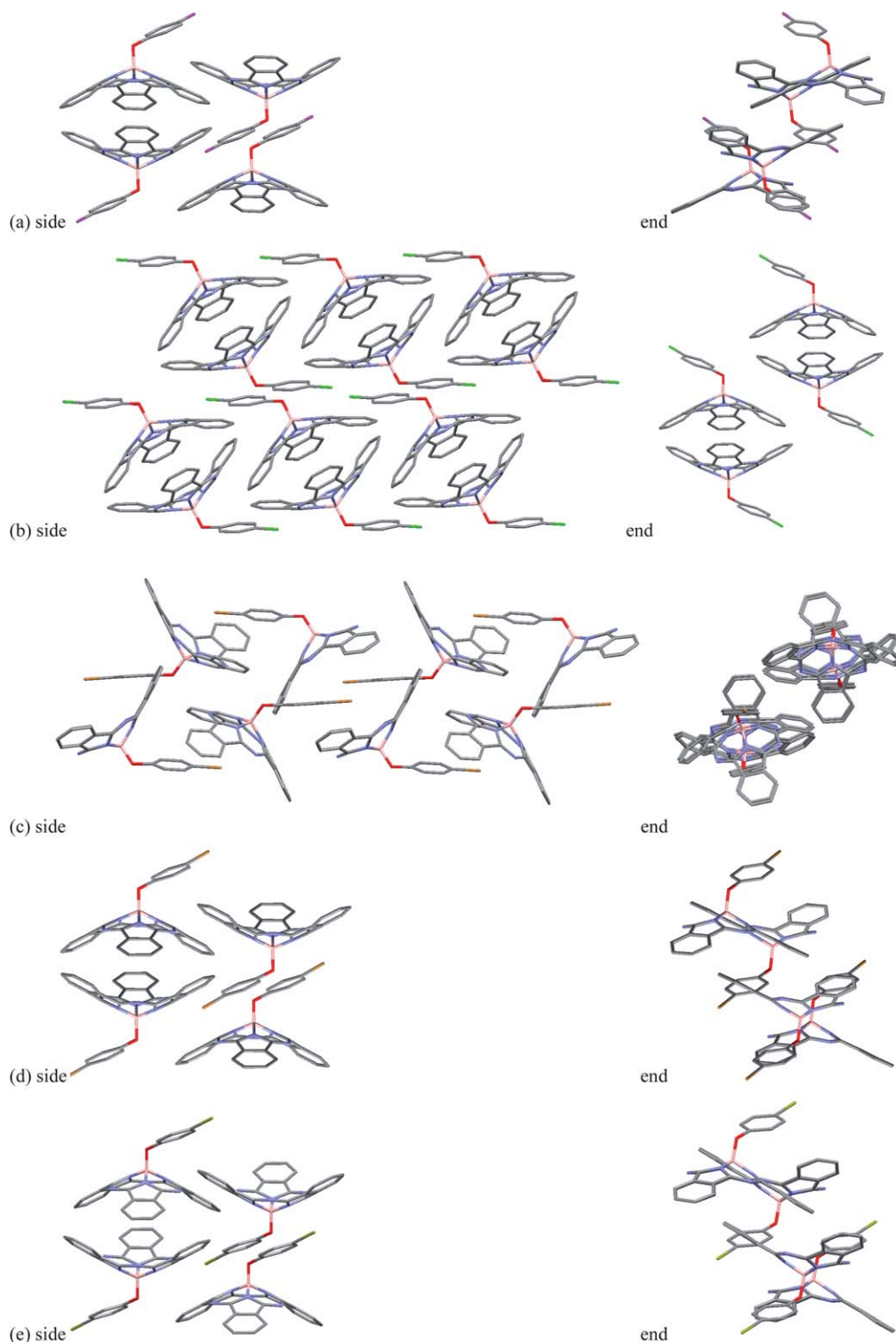


**Fig. 1** Illustration of the molecular packing arrangement within the single crystal (extended beyond the unit cell) of (a) FPhO-**BsubPc**, (b) ClPhO-**BsubPc**, (c)  $\alpha$ -BrPhO-**BsubPc**, (d)  $\beta$ -BrPhO-**BsubPc** and (e) IPhO-**BsubPc**. Colours: carbon = grey; nitrogen = blue; boron = light brown; fluorine = violet; chlorine = green; bromine = yellow; iodine = dark brown. Hydrogens omitted for clarity. (a) Redrawn from ref. 3.

fragment and the halogen atom but rather the unique combination of the electrostatics of the molecule, the size of the bromine atom and the size of the underside of the bowl of the **BsubPc** ligand which leads to the formation of this new molecular packing arrangement. This new packing motif does place the phenoxy fragment over a lobe of the

**BsubPc** ligand; it can be formed without placing strain on the bond angles within the **BrPhO-BsubPc** molecule.

In summary, we have observed a new crystal packing motif for **BsubPcs**. This different packing structure occurs only in the case of **BrPhO-BsubPc** and not for the other *para*-halophenoxy-**BsubPcs**

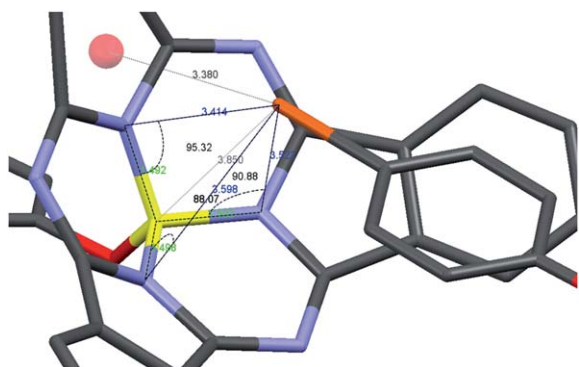


**Fig. 2** Illustration of the area of the bromine atom and the boron of its nearest neighbour in  $\alpha$ -BrPhO-BsubPc.

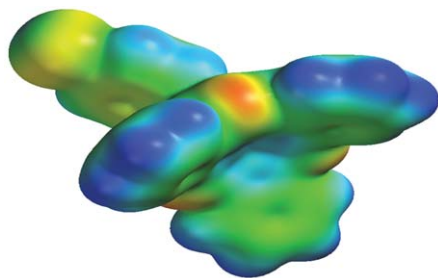


**Fig. 3** Electrostatic potential 3D mapped isosurface plot of BrPhO-BsubPc generated using the 6-31G\* basis set with the B3LYP DFT method. Areas of electron deficiency are coloured blue; areas of electron excess are colored red.

presented in this study. Given the similar electrostatic distributions for all compounds in this study, we must conclude the unique motif observed ( $\alpha$ -BrPhO-BsubPc) is a result of the combination of the electrostatics and the particular size of the bromine atom giving a favourable  $\pi$ -Br interaction that directs its solid-state packing. Based on computer aided modelling, indications are that this new form is a kinetically favoured polymorph.

## Notes and references

‡ For a description of the terminology used to describe BsubPcs, specifically concave and convex face, see ref. 1.

§ Crystal data for  $\alpha$ -BrPhO-BsubPc:  $C_{30}H_{16}BBrN_6O$ ,  $M = 567.21$ , monoclinic,  $a = 15.7312(12)$  Å,  $b = 10.2246(9)$  Å,  $c = 16.4141(13)$  Å,  $\alpha = 90^\circ$ ,  $\beta = 113.281(5)^\circ$ ,  $\gamma = 90^\circ$ ,  $V = 2425.2(3)$  Å<sup>3</sup>,  $T = 150(1)$  K, space group  $P2_1/n$ ,  $Z = 4$ , 14 248 reflections measured, 5448 independent reflections ( $R_{int} = 0.0961$ ). The final  $R_1$  value was 0.0638 ( $I > 2\sigma(I)$ ). The final  $wR(F^2)$  value was 0.1388 ( $I > 2\sigma(I)$ ). The final  $R_1$  value was 0.1368 (all data). The final  $wR(F^2)$  values were 0.1690 (all data).

¶ Crystal data for  $\beta$ -BrPhO-BsubPc:  $C_{30}H_{16}BBrN_6O$ ,  $M = 567.21$ , triclinic,  $a = 10.1389(4)$  Å,  $b = 11.0056(4)$  Å,  $c = 11.6749(5)$  Å,  $\alpha = 86.929$

( $2^\circ$ ),  $\beta = 78.811(2)^\circ$ ,  $\gamma = 68.0100(19)^\circ$ ,  $V = 1184.74(8)$  Å<sup>3</sup>,  $T = 150(1)$  K, space group  $P\bar{1}$ ,  $Z = 2$ , 12 718 reflections measured, 5379 independent reflections ( $R_{int} = 0.0437$ ). The final  $R_1$  value was 0.0413 ( $I > 2\sigma(I)$ ). The final  $wR(F^2)$  value was 0.0906 ( $I > 2\sigma(I)$ ). The final  $R_1$  value was 0.0659 (all data). The final  $wR(F^2)$  value was 0.1009 (all data).

- C. G. Claessens, D. González-Rodríguez, B. del Rey and T. Torres, *Chem. Rev.*, 2002, **102**, 835–853.
- (a) C. G. Claessens, D. González-Rodríguez, T. Torres, F. Agulló-López, I. Ledoux, J. Zyss, V. R. Ferro and J. M. G. de la Vega, *J. Phys. Chem. B*, 2005, **109**, 3800–3806; (b) G. E. Morse, M. G. Helander, J. F. Maka, Z. H. Lu and T. P. Bender, *ACS Appl. Mater. Interfaces*, 2010, **2**(7), 1934–1944; (c) D. D. Díaz, H. J. Bolink, L. Cappelli, C. G. Claessens, E. Coronado and T. Torres, *Tetrahedron Lett.*, 2007, **48**, 4657–4660; (d) K. L. Mutolo, E. I. Mayo, B. P. Rand, S. R. Forrest and M. E. Thompson, *J. Am. Chem. Soc.*, 2006, **128**, 8108–8109; (e) H. Kumar, P. Kumar, R. Bhardwaj, G. D. Sharma, S. Chand, S. C. Jain and V. Kumar, *J. Phys. D: Appl. Phys.*, 2009, **42**, 015103; (f) H. Gommans, D. Cheyns, T. Aernouts, C. Giroto, J. Poortmans and P. Heremans, *Adv. Funct. Mater.*, 2007, **17**, 2653–2658; (g) T. Yasuda and T. Tsutsui, *Mol. Cryst. Liq. Cryst.*, 2007, **462**, 3–9; (h) H. Gommans, T. Aernouts, B. Verreet, P. Heremans, A. Medina, C. G. Claessens and T. Torres, *Adv. Funct. Mater.*, 2009, **19**, 3435–3439.
- A. S. Paton, G. E. Morse, A. J. Lough and T. P. Bender, *CrystEngComm*, 2011, **13**, 914, DOI: 10.1039/C0CE00599A.
- R. Potz, M. Goldner, H. Huckstadt, U. Cornelissen, A. Tutass and H. Homborg, *Z. Anorg. Allg. Chem.*, 2000, **626**, 588–596, CCDC reference KAJPEQ.
- K. Kasuga, T. Idehara, M. Handa, Y. Ueda, T. Fujiwara and K. Isa, *Bull. Chem. Soc. Jpn.*, 1996, **69**, 2559–2563, CCDC reference RUGJOS.
- Y. Inokuma, J. H. Kwon, T. K. Ahn, M. C. Yoo, D. Kim and A. Osuka, *Angew. Chem., Int. Ed.*, 2006, **45**, 961–964, CCDC reference PEFWAZ.
- M. K. Engel, J. Yao, H. Maki, H. Takeuchi, H. Yonehara and C. Pac, *Rep. Kawamura Institute of Chem. Res.*, 1997, **9**, 53, CCDC reference UCJIOF.
- C. G. Claessens and T. Torres, *Angew. Chem., Int. Ed.*, 2002, **41**, 2561–2677.
- A. S. Paton, G. E. Morse, J. F. Maka, A. J. Lough and T. P. Bender, *Acta Crystallogr., Sect. E: Struct. Rep. Online*, 2010, **66**, o3059.
- M. D. Prasanna and T. N. Guru Row, *Cryst. Eng.*, 2000, **3**, 135–154.
- R. K. R. Jetti, A. Nangia, F. Xue and T. C. W. Mak, *Chem. Commun.*, 2001, 919–920.
- A. Noman, M. M. Rahman, R. Bishop, D. C. Craig and M. L. Scudder, *CrystEngComm*, 2003, **5**(75), 422–428.
- C. Bustos, C. Sanchez, E. Schott, M. T. Garland and L. Alvarez-Thon, *Acta Crystallogr., Sect. E: Struct. Rep. Online*, 2006, **62**, m3104–m3106.
- T. Fukuda, J. R. Stork, R. J. Potucek, M. M. Olmstead, B. C. Noll, N. Kobayashi and W. S. Durfee, *Angew. Chem., Int. Ed.*, 2002, **41**, 2565–2568.
- G. E. Morse, J. F. Maka, A. J. Lough and T. P. Bender, *Acta Crystallogr., Sect. E: Struct. Rep. Online*, 2010, **66**, o3057–o2974.
- M. S. Rodriguez-Morgade, C. G. Claessens, A. Medina, D. Gonzalez-Rodríguez, E. Gutierrez-Puebla, A. Monge, I. Alkorta, J. Elguero and T. Torres, *Chem.–Eur. J.*, 2008, **14**, 1342–1350.
- A. Bondi, *J. Phys. Chem.*, 1964, **68**, 441–451.